



**HAL**  
open science

## Modeling of a Liquid–Liquid–Solid Heterogeneous Reaction System: Model System and Peroxyvaleric Acid

Sébastien Leveneur, Cesar A de Araujo Filho, Lionel Estel, Tapio Salmi

### ► To cite this version:

Sébastien Leveneur, Cesar A de Araujo Filho, Lionel Estel, Tapio Salmi. Modeling of a Liquid–Liquid–Solid Heterogeneous Reaction System: Model System and Peroxyvaleric Acid. *Industrial and engineering chemistry research*, 2012, 51 (1), pp.189-201. 10.1021/ie2017064 . hal-02151570

**HAL Id: hal-02151570**

**<https://normandie-univ.hal.science/hal-02151570v1>**

Submitted on 21 Dec 2021

**HAL** is a multi-disciplinary open access archive for the deposit and dissemination of scientific research documents, whether they are published or not. The documents may come from teaching and research institutions in France or abroad, or from public or private research centers.

L'archive ouverte pluridisciplinaire **HAL**, est destinée au dépôt et à la diffusion de documents scientifiques de niveau recherche, publiés ou non, émanant des établissements d'enseignement et de recherche français ou étrangers, des laboratoires publics ou privés.

Modelling of a liquid-liquid-solid heterogeneous reaction system: Model system  
and peroxyvaleric acid

*Sébastien Leveneur<sup>a,b\*</sup>, Cesar A. de Araujo Filho<sup>a</sup>, Lionel Estel<sup>b</sup>, Tapio Salmi<sup>a</sup>*

<sup>a</sup>Laboratory of Industrial Chemistry and Reaction Engineering, Process Chemistry Centre, Åbo Akademi University, Biskopsgatan 8, FI-20500 Åbo/Turku, Finland.

<sup>b</sup>LSPC-Laboratoire de Sécurité des Procédés Chimiques, INSA Rouen, BP08, Avenue de l'Université, 76801 Saint-Etienne-du-Rouvray, France.

Tel: +33 2 32 95 66 54; Fax: +33 2 32 95 66 52; E-mail: sebastien.leveneu@insa-rouen.fr

---

ABSTRACT

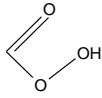
A mathematical model was developed to interpret a liquid-liquid-solid heterogeneous reaction system using valeric acid (pentanoic acid) perhydrolysis as model. Kinetic, thermodynamic and mass transfer parameters were included in this model. Perhydrolysis of valeric acid (pentanoic acid) on Amberlite IR-120 catalyst experiments were carried out in the temperature range of 40-60°C and with an initial valeric acid concentration of 50 wt.%. The influence of water and the acid catalyst was taken into account to develop a suitable kinetic model. The thermodynamic parameters, such as the reaction enthalpy ( $\Delta H_r^0$ ) and the molar equilibrium ratio ( $m$ ) were determined experimentally. The kinetic parameters were determined by non-linear regression analysis and they were statistically well-identified. The standard reaction enthalpy was estimated to  $-13.84 \text{ kJ}\cdot\text{mol}^{-1}$  and the activation energy of the reaction was estimated to  $64.5 \text{ kJ}\cdot\text{mol}^{-1}$ .

Keywords: Kinetics, mathematical modelling, liquid-liquid-solid system, solid acid catalyst.

---

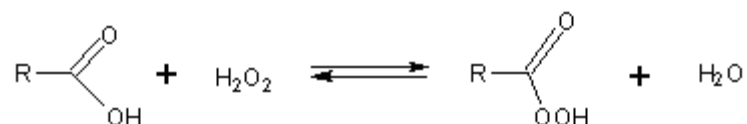
## 1. Introduction

Peroxy-carboxylic acids are widespread in industry, for instance 10,000 tonnes worldwide were produced in 2002 [1]. Three application domains for peroxy-carboxylic acids can be distinguished: disinfecting agents, bleaching agents and as intermediates in fine chemistry. All these applications are based on the

oxidative properties of these compounds, due to the chemical bond . The literature concerning the synthesis of short-chain peroxy-carboxylic (3-1 carbon atoms) acid is relatively extensive with homogeneous [2-9] and heterogeneous catalysts [10-18]. Indeed, they are the main peroxy-carboxylic acids used in industrial scale, mainly because of their high reactivity and so lower stability. On the other hand, studies of peroxy-carboxylic acids with long carbon chains (higher than 4 carbons) are rare [19-20]. These long-chain peroxy-carboxylic acids can be used, when the solubility of a short-chain peroxy-carboxylic acid or hydrogen peroxide in the organic phase is limited. An application of peroxyfatty acid concerns washing powders, in which their role is to release hydrogen peroxide to allow its bleaching action in the organic phase.

The synthesis of peroxy-carboxylic acids is based on the oxidation of the parent carboxylic acid. In industry, such oxidation reactions are fundamental, but many of these reactions are carried out by using conventional heavy-metal oxidants, which form toxic waste, application of nitric acid, which form the greenhouse gas  $N_2O$ ; and utilization of molecular oxygen, which requires safety precautions and could cause over-oxidation. According to Noyori [21], an elegant way to surmount these

problems is the use of aqueous hydrogen peroxide, as hydrogen peroxide is a powerful oxidant. The production of peroxy-carboxylic acid involves the use of hydrogen peroxide and carboxylic acid as reactants, thus avoiding the use of oxygen. This liquid-phase reaction is called perhydrolysis, and can be described as follows:



This reaction is governed by thermodynamics; a typical value of the equilibrium constant is 2.39 for acetic acid at 30°C. As illustrated by Figure 1, increasing the carbon chain length, the kinetics of this reaction becomes retarded [18]. The shortest peroxy-carboxylic acid, peroxyformic acid is formed spontaneously from formic acid and hydrogen peroxide, but an added acid catalyst is needed for the synthesis of long-chain peroxy-carboxylic acids.

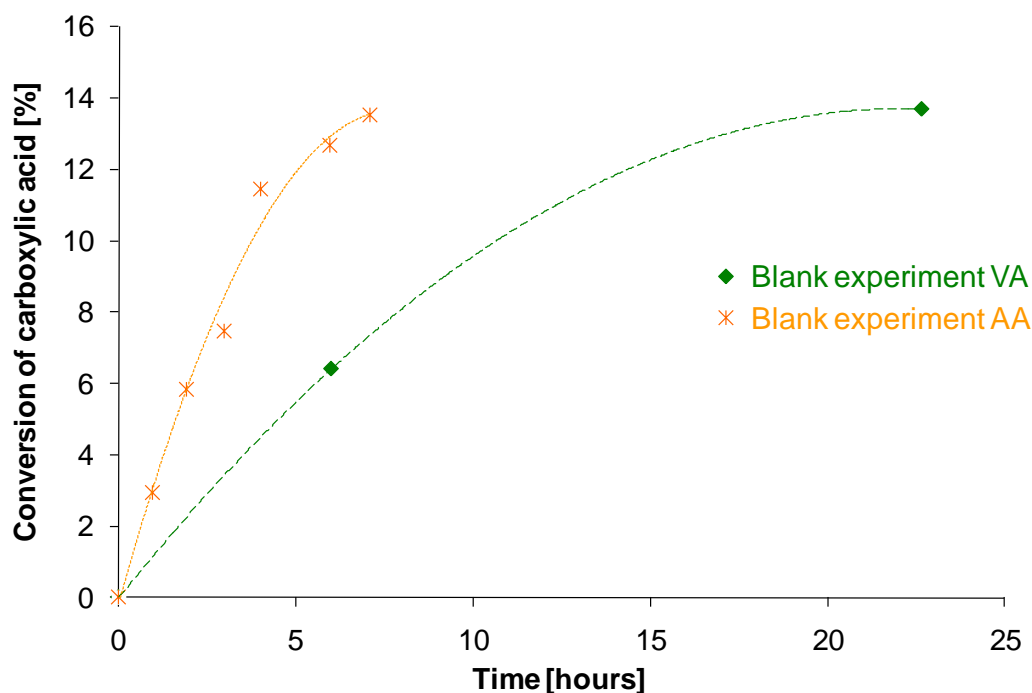


Figure 1. Blank experiments carried out with acetic and valeric acid at 60°C.

The motivation of such study is that long chain carboxylic acid and derivatives are produced from biomass valorization leading to liquid heterogeneous reaction system in presence of aqueous phase. In such system, equilibrium study is an important issue to understand the distribution of the chemicals between phases; mass transfer study allows characterizing the interfacial flux of chemical and a kinetic study is needed to follow the course of the reaction. The goal of this paper was to include all these parameters in a mathematical model to describe a liquid-liquid-solid heterogeneous reaction system.

The synthesis of peroxyvaleric acid from hydrogen peroxide and valeric acid (pentanoic acid) was selected as a model system, because the kinetic mechanism of carboxylic acid perhydrolysis has been studied by our research group [9, 16, 18]. The clear benefit of this acid is to be non-miscible in aqueous phase allowing a simple and rapid separation of the aqueous and organic phases.

## 2. EXPERIMENTAL SECTION

### 2.1 Reactor and system

The experiments were carried out in a batch reactor equipped with a mechanical stirrer and a temperature probe. On top of the reactor, a cooling condenser was placed, and adjusted at 0°C to avoid volatilization of the liquid-phase compounds. In case that decomposition of peroxyvaleric acid (PVA) or H<sub>2</sub>O<sub>2</sub> appeared, a carrier gas (Helium) was led into the reactor through one of the reactor necks to prevent accumulation of oxygen in the gas phase. A pitched blade impeller (PTFE coated) was used to ensure vigorous mixing during the reaction.

To prevent contamination induced by alkaline and metal components, which could initiate the catalytic decomposition of peroxyvaleric acid and hydrogen peroxide, all parts of the reactor system being in contact with the reaction solution were washed with hydrochloric acid followed by another washing, with a phosphate-free detergent solution.

Two different addition procedures were tested to reveal their influence on the reaction kinetics. In the first procedure, valeric acid (Acros, 99 wt.%) and the dried catalyst were added into the reactor until the desired reaction temperature was reached, and then aqueous hydrogen peroxide solution (Merck, 30 wt.%) was fed through the dropping funnel. The second procedure consisted to add the aqueous hydrogen peroxide solution and the dried catalyst into the reactor, and when the desired temperature was reached, the valeric acid solution was fed rapidly into the

reactor. The time “zero” was defined when the dropping funnel was opened. The solution was fed in 30 seconds from the funnel in the reactor.

Table 1 introduces the experimental matrix for the synthesis in the presence of heterogeneous catalysts.

Table 1. Experimental conditions

Reaction temperature	40-60°C
Rotator speed	200-800 rpm
Initial amount of valeric acid	20-84 wt.%
Initial amount of (H <sub>2</sub> O + H <sub>2</sub> O <sub>2</sub> )	16-80 wt.%
Catalyst (Amberlite) loading on dried basis	0-29 g
Reaction volume	250 ml

## 2.2 Sampling

In order to follow the reaction kinetics, several samples from the liquid mixture were withdrawn and analyzed at different times. Due to the short time of separation (ca. 1 min) of the different phases after stopping the agitation, it was possible to analyze a sample from the aqueous and organic phases.

## 2.3 Chemical analysis

The liquid phase was analyzed off-line by titration with the Greenspan and Mackellar methods [22]. The concentration of hydrogen peroxide was determined by titration using a standard solution of ammonium cerium sulfate (0.1 N). The concentrations of carboxylic and peroxy-carboxylic acids were determined by

titration with an automatic titrator (Metrohm 751 GPD Titrino) by using a standard solution of sodium hydroxide (0.2 N).

## 2.4 Catalyst analysis

Cation exchange resins were used as solid acid catalysts, namely Amberlite IR-120 and Dowex. These resins are cation exchange resins with a styrene-divinyl benzene matrix bearing sulfonic acid groups, and they are very similar (Table 2). The catalyst was used in the form of beads. Amberlite IR-120 was used for the kinetic and equilibrium experiments, and Dowex to study the influence of the internal mass transfer.

Table 2. Properties of the cation exchange resin

	Polymer type	Cross linking % DVB	Moisture content % mass	Capacity meq/g	Particle size range mm
Amberlite IR-120	Gel type	8	45	4,4	0.3-1.2
Dowex 50Wx8-400	Gel type	8	54	4,8	0.04-0.08
Dowex 50Wx8-50	Gel type	8	55	4,8	0.3-0.84

Prior to the experiment, the native resin was washed with a hydrogen peroxide solution (10 wt. %) and de-ionised water. Then, the catalyst was dried for 24 hours at 99°C. The purpose of this pre-treatment was to remove the impurities from the resins and to know the exact mass of catalyst, i.e., based on dried basis, introduced into the reactor.

At the end of the experiments, the catalyst was filtrated a first time to remove the residual interstitial liquid between the particles. Then, the catalyst was filtrated several times with deionised water, and the filtrated fluid was analyzed. By using this method, it was possible to estimate the average concentration of carboxylic acid, peroxy-carboxylic acid and hydrogen peroxide remaining inside the catalyst.



### 3. Results and discussions

The determination of the continuous and dispersed phases is crucial in such a system. By using the conductivity method, it was found that for a weight percentage of valeric acid less than 45 %, the continuous phase was the aqueous one. On the opposite, when the weight percentage of valeric acid exceeded 45 %, then the continuous phase was the organic one.

Experimental results show that the consumed reactants were valeric acid from the organic phase and hydrogen peroxide from the aqueous one, but not valeric acid from the aqueous phase and hydrogen peroxide from the organic phase, whose concentrations remained practically constant during the reaction. By using the analytical method described in the previous section, peroxyvaleric acid was detected only in the organic phase. These observations were noticed in the presence and absence of the catalyst, at any temperature and composition of the continuous phase.

Preliminary analysis indicated, which reactant from which phase was consumed and the composition of the continuous phase with respect to the initial amount of the valeric acid. The amount and nature of the dispersed phase can play an important role on the interfacial tension, leading to different drop size distribution, on the polarity of the reaction mixture, leading to different equilibrium stage, and on the swelling of the catalyst particle leading to different particle size distributions [16-17]. For the sake of simplicity, these parameters, i.e., polarity, interfacial tension and swelling effect were kept constant by using the same initial ratio of valeric acid and the aqueous solution. Thus, only the ratio  $\text{H}_2\text{O}_2:\text{H}_2\text{O}$  was different.

An initial value of 50 wt.% of valeric acid was used, because the reaction kinetics and the equilibrium conversion of valeric acid were found to be optimal (Figure 2), and the two liquid phases were rapidly separated after the end of the agitation.

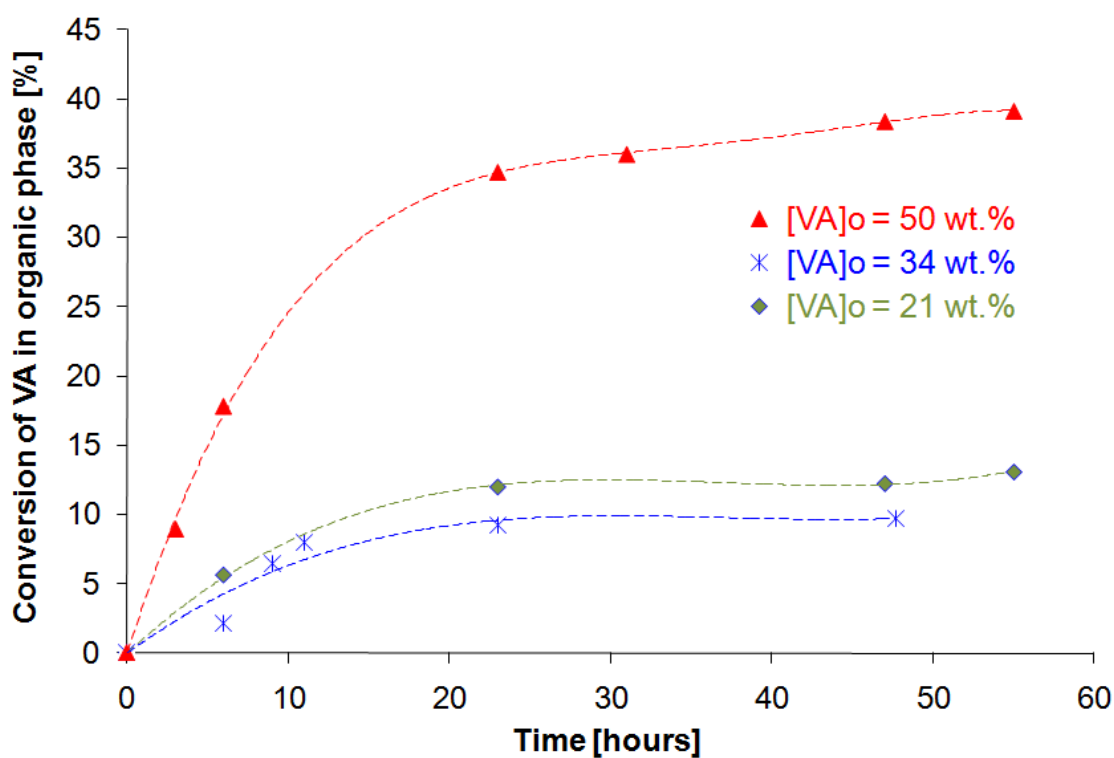


Figure 2. Conversion of valeric acid in the organic phase at 40°C catalysed by Amberlite IR-120.

By using an initial weight percent of valeric acid equal to 50 %, the dispersed phase was the aqueous phase, while the continuous phase was the organic one.

### 3.1. Equilibrium analysis

#### 3.1.1. Chemical equilibrium

Perhydrolysis reactions, such as esterification reactions, are governed by the equilibrium constant. Bucalà et al. [23] have demonstrated that in case of a liquid-liquid system, the thermodynamic equilibrium constant in the organic and aqueous phases are equal:

$$K_{org}^T = K_{aq}^T = \frac{\sum a_{org}^{Products}}{\sum a_{org}^{Reactants}} = \frac{\sum a_{aq}^{Products}}{\sum a_{aq}^{Reactants}} \quad (1)$$

where  $a$  stands for the activity of compounds.

To determine the thermodynamic parameters, e.g., the equilibrium constant and the reaction enthalpy, the methodology described in the previous papers of our group was followed [9, 16]. The other aim of such experiments was to determine the distribution parameter ( $m$ ) of the different compounds between the organic and aqueous phases at different temperatures.

The true thermodynamic constant  $K^T$  follows the law of Van't Hoff:

$$\frac{d \ln K^T}{dT} = \frac{\Delta H_r^0}{RT^2} \quad (2)$$

where  $\Delta H_r^0$  stands for the standard reaction enthalpy. Approximating that  $\Delta H_r^0$  is independent of  $T$ , integration of eq 2 from a particular temperature ( $T_{ref}$ ) to an arbitrary one ( $T$ ) leads to

$$\ln \frac{K^T}{K_{ref}^T} = \frac{-\Delta H_r^0}{R} \left( \frac{1}{T} - \frac{1}{T_{ref}} \right) \quad (3)$$

To check the validity of eq 3 at different temperatures, the polarity of the experiments was the same by keeping the same initial amount of valeric acid (50 wt.%), aqueous compounds (H<sub>2</sub>O+H<sub>2</sub>O<sub>2</sub>) and catalyst loading (49 g/l).

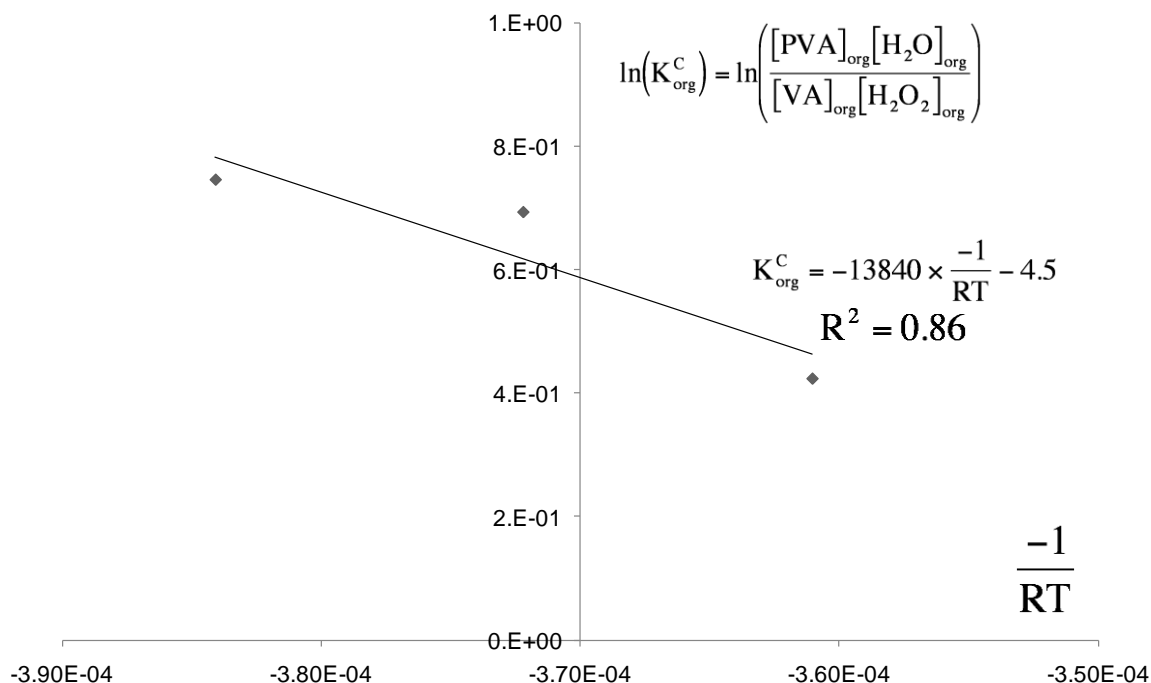


Figure 3. Plot  $\ln(K^{\text{C}})$  versus  $-1/RT$ .

Figure 3 shows that valeric acid perhydrolysis follows the law of van't Hoff similarly to the perhydrolysis of acetic and propionic acid perhydrolysis [9, 16]. With an initial amount equal to 50 wt.% of valeric acid, the reaction enthalpy was found to be -13.84 kJ/mol. However, it should be kept in mind that the equilibrium constant displayed by Figure 3 was obtained by using the concentrations of the compounds in the organic phase and not their activities. The concentration-based equilibrium constant, denoted by  $K^{\text{C}}$ , was used in the kinetic model, using eq 3. This simplification was possible, because all the experiments were carried out with the same amount of valeric acid, and thus the polarities of these solutions were the same.

### 3.1.2. Determination of the distribution coefficients

The distribution coefficients or equilibrium molar ratios depend on the temperature and polarity of the reaction system, as the thermodynamic equilibrium constants.

The distribution coefficients of the different species were defined as

$$m(i) = \frac{[i]_{\text{org}}^*}{[i]_{\text{aq}}^*} \approx \left( \frac{[i]_{\text{org}}}{[i]_{\text{aq}}} \right)_{\text{at the equilibri}} \quad (4)$$

The liquid-liquid equilibrium is a thermodynamic equilibrium. Thus, the distribution constants  $m(i)$  can be related to the Gibbs energy of distribution:

$$m(i) = \exp\left(\frac{-\Delta G_d}{RT}\right) \quad (5)$$

By applying the law of Van't Hoff, it is possible to obtain

$$\ln \frac{m(i)_T}{m(i)_{T_{\text{ref}}}} = \frac{-\Delta H_d^0}{R} \left( \frac{1}{T} - \frac{1}{T_{\text{ref}}} \right) \quad (6)$$

This approximation evolves that  $\ln m(i)_T$  versus  $\frac{-1}{RT}$  is a straight line (Figure 4).

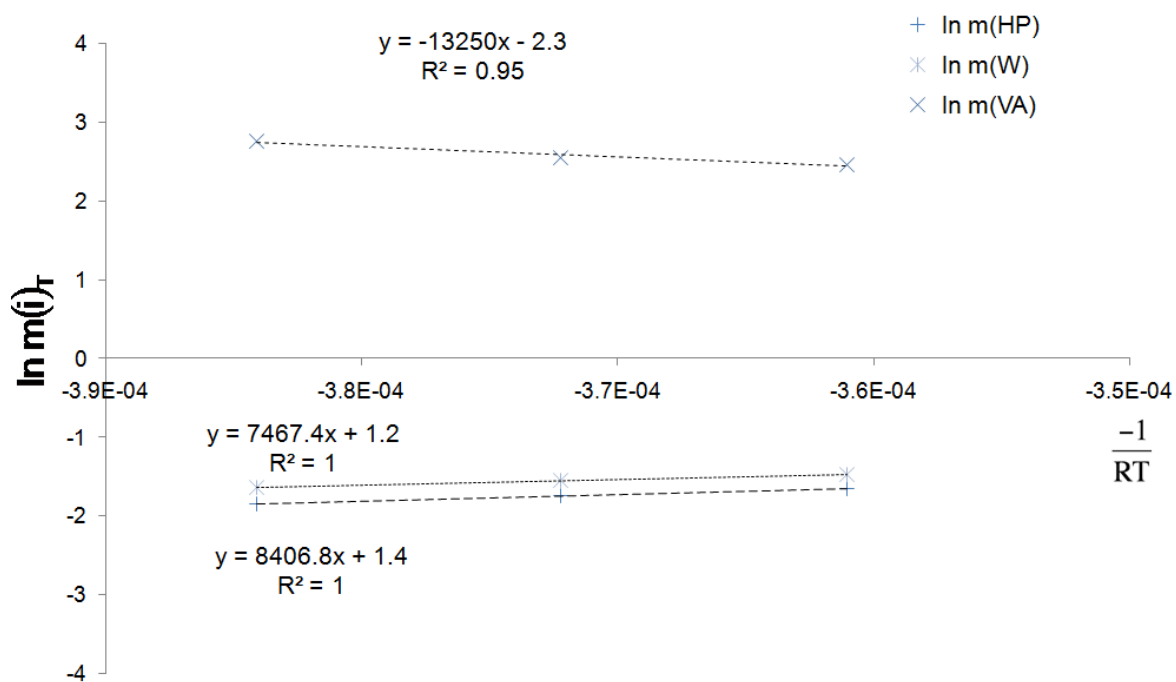


Figure 4. Plot of  $\ln m(i)_T$  versus  $\frac{-1}{RT}$  with a solution of 50 wt. % of valeric acid and catalyst loading of 45 g.l<sup>-1</sup>.

Figure 4 shows that the distribution of hydrogen peroxide, water and valeric acid between organic and aqueous phase are antagonist. Indeed, increasing the temperature leads to decrease the concentration of valeric acid in the organic phase, and vice-versa for hydrogen peroxide and water. The equations for the equilibrium constant (eq 3) and distribution coefficient (eq 6) were included in the model.

### 3.2. Catalyst concentration

It was found that the concentrations inside the catalyst particle were not affected by the reaction temperature or catalyst loading up to the value of 110 g/l. However, these values are strongly dependent on the organic and aqueous bulk-phase concentrations as illustrated by Figure 5. A linear dependence between the hydrogen peroxide concentration in the bulk and particle phases was detected. The initial amount of valeric acid was maintained constant during the experiments; thus, the concentration variations are less pronounced. The concentrations inside the particle can thus be approximated by the following relation:

$$\left. \begin{aligned} [\text{H}_2\text{O}_2]_p &= \alpha [\text{H}_2\text{O}_2]_{\text{aq}} \\ [\text{H}_2\text{O}]_p &= \alpha [\text{H}_2\text{O}]_{\text{aq}} \\ [\text{VA}]_p &= \beta [\text{VA}]_{\text{aq}} \\ [\text{PVA}]_p &= \beta [\text{PVA}]_{\text{aq}} \end{aligned} \right\} \quad (7)$$

In the system of eqs 7, valeric-peroxyvaleric acids and water-hydrogen peroxide were assumed to have similar behaviour towards absorption, for that reason they were approximated to have the same coefficient of absorption  $\alpha$  and  $\beta$ . These parameters were assumed to be temperature independent within the range of 40-60°C.

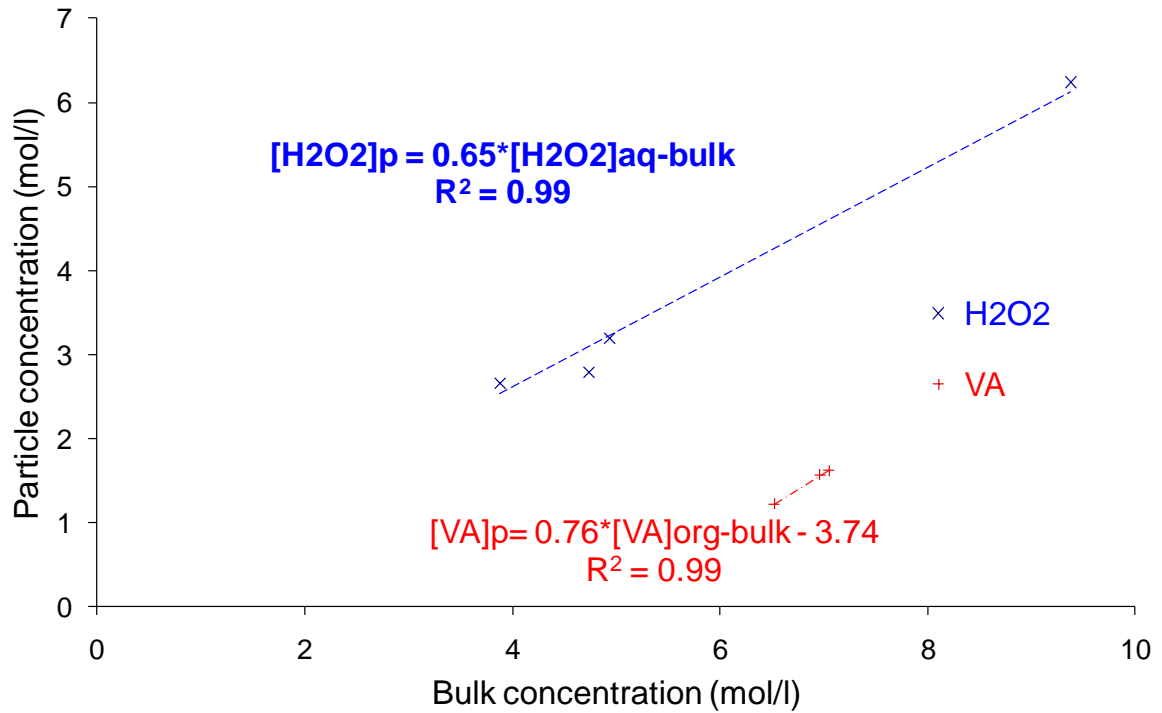


Figure 5. Relationship between the bulk aqueous and bulk organic phase concentrations and particle concentrations with  $[VA]_o$ : 50 wt.%.

Figure 5 shows that y-intercept term is not equal to zero in case of valeric acid absorption equation. This is due to the fact that the concentration of valeric acid was in the same range of order during this study. The equation system (7) was included in the kinetic model to get the intrinsic rate constant.



### 3.3 Mass transfer study

According to the experimental results, peroxyvaleric acid (PVA) was detected only in the organic phase. From the kinetic curves, it was observed that valeric acid from the organic phase and hydrogen peroxide from the aqueous phase were consumed during the reaction.

In the case of peroxyvaleric acid synthesis from valeric acid and hydrogen peroxide by resins, there are two distinguished mechanisms of catalysis the homogeneous one ( $r_{\text{hom}}$ ) and the heterogeneous one ( $r_{\text{het}}$ ). The homogeneous mechanism is due to the dissociation of valeric acid producing hydroxonium ions and the heterogeneous one is due to the active sites of the sole resin catalyst. The initial amount of valeric acid was fixed to be 50 wt. %, thus the continuous phase is the organic phase. To study the mass transfer effect in such a liquid-liquid-solid system, the mass transfer coefficient for the continuous phase ( $k_c$ ), the dispersed phase ( $k_d$ ) and the solid phase ( $k_p$ ) should be taken into account. From literature [24-26], it is well known that several parameters could affect the kinetics of a liquid-liquid-solid heterogeneous reaction system, such as the shape of the impeller, the impeller-diameter-to-reactor-diameter, the position of the impeller towards the reactor bottom, baffled or un-baffled reactor, the viscosity of the reaction mixture, etc. In the present case, the influence of the rotating speed and catalyst particle size was investigated.

In order to establish the different mass balance equations governing the system, the following assumptions were done:

- production of PVA due to the dissociation of the valeric acid occurs in the organic and aqueous phase (homogeneous catalysis),
- production of PVA due to the dissociation of the valeric acid was considered to be negligible inside the particle (homogeneous catalysis in the catalyst pores),
- water and hydrogen peroxide from the aqueous phase diffuse to the organic phase and to the particle,
- valeric acid from the organic phase diffuses to the aqueous phase and to the particle,
- peroxyvaleric acid from the particle diffuses to the organic bulk phase.

Figure 6 shows the different mass transfer phenomena, which take place during the reaction based on the film theory.

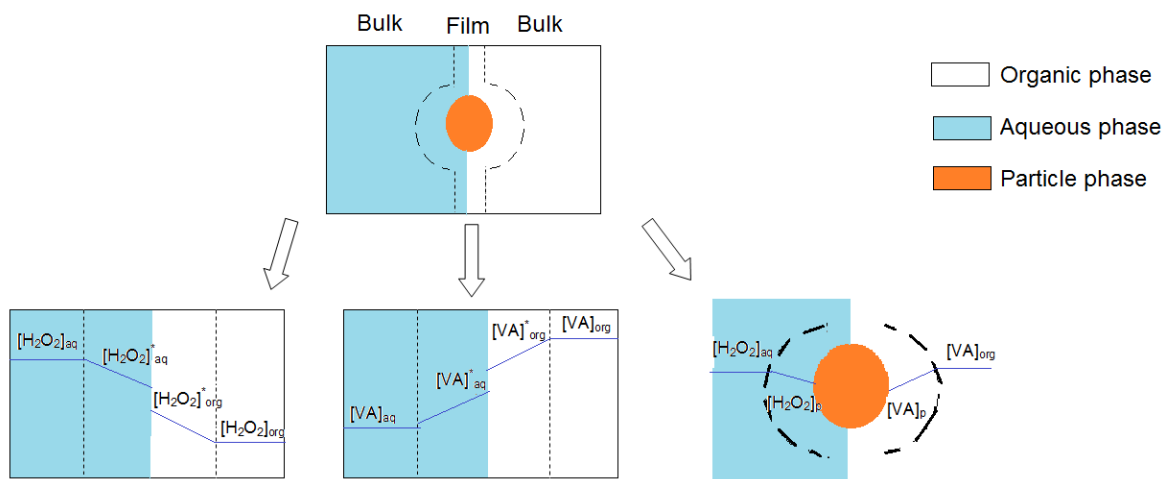


Figure 6. Concentration profiles of hydrogen peroxide and valeric acid in the liquid-liquid-solid system.

### 3.3.1 Influence of the rotating speed on the reaction velocity

As described in the Experimental section, a pitched blade impeller was used to ensure a vigorous mixing. To suspend the particles, a rotating speed exceeding 50 rpm was necessary. Similar experiments were carried out at different rotating speeds ranging from 200 to 800 rpm. Based on this experiment, it was found that the influence of the agitation speed on the kinetics can be assumed negligible.

### 3.3.2 Influence of the internal mass transfer

To measure the importance of the internal mass transfer, which is different from the swelling effect, different catalyst particle diameters were used. Instead of using Amberlite IR-120, two different size ranges of Dowex 50Wx8 were used: Dowex 50Wx8-400 (0.04-0.08 mm) and Dowex 50Wx8-50 (0.3-0.84 mm). By using Dowex and Amberlite catalysts, it was possible to determine the influence of the internal mass transfer resistance. Both catalysts are chemically similar (Table 2). It was found that the effect of internal mass transfer is negligible for this reaction system. In the case of the synthesis of peroxyacetic and peroxypropionic acid carried out with the same heterogeneous catalyst, internal mass transfer limitation was found to be non-negligible [16-17]; this might be due to the faster kinetics with short carbon-chain carboxylic acids perhydrolysis [18]. The absence of internal mass transfer resistance does not imply that there might not be a gradient of the concentrations between the bulk and particle phases. In case of resins, a swelling effect is present [14, 27], which is caused by the fact that water is preferentially adsorbed than other compounds, leading to an increase of the particle size.

### 3.4. Kinetic study

Based on the previous study [16], the perhydrolysis reaction in the presence of cation exchange resins consists of two different parts: the self-catalyzed reaction due to the protolysis of carboxylic acid (homogeneous catalysis) and the Eley-Rideal mechanism with the adsorption of the carboxylic acid on the sulfonic group (heterogeneous catalysis).

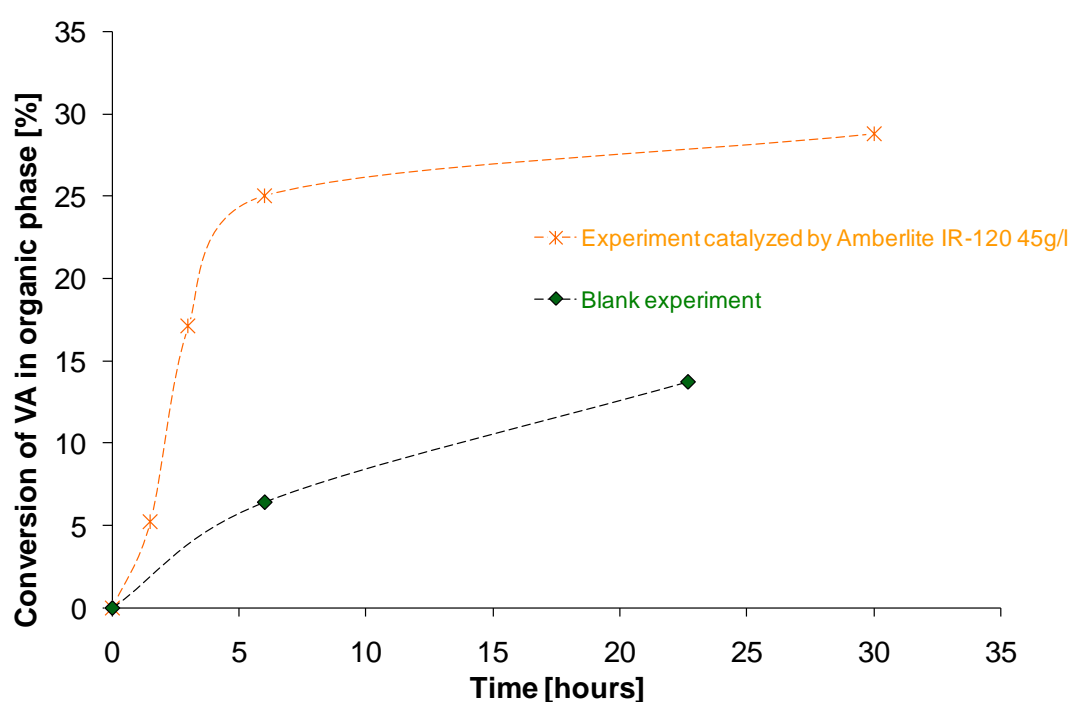


Figure 7. Conversion of valeric acid in the presence and absence of the heterogeneous acid catalyst at 60°C.

Figure 7 shows that one cannot neglect the influence of the self-catalyzed reaction during the synthesis of peroxyvaleric acid from valeric acid and hydrogen peroxide.

A detailed derivation of the kinetic equations can be found in the previous paper of our group [16], in which an Eley-Rideal mechanism was used assuming the adsorption of the carboxylic acid molecules on the active site of the catalyst.

The heterogeneously catalyzed reaction rate is expressed with the particle concentrations as

$$r_{\text{het}} = \frac{k_{\text{het}} \times [-\text{SO}_3\text{H}]_p}{1 + K_{\text{VA and PVA adsorption}}^C \times ([\text{VA}]_p + [\text{PVA}]_p) + K_{\text{Water adsorption}}^C \times [\text{H}_2\text{O}]_p} \times \left( [\text{VA}]_p \times [\text{H}_2\text{O}_2]_p - \frac{1}{K_{\text{het}}^C} \times [\text{PVA}]_p \times [\text{H}_2\text{O}]_p \right) \quad (8)$$

where the subscript (p) states for the catalyst particle. The concentration  $[-\text{SO}_3\text{H}]_p$  is the amount of sulfonic acid groups per liquid volume inside the particle (Table 2). The concentrations of the carboxylic and peroxycarboxylic acid, hydrogen peroxide and water were calculated by using the equation system (7). The value for the adsorption coefficient of water  $K_{\text{water adsorption}}^C$  was calculated based on the equation developed by Altiokka [28]. The kinetic constant  $k_{\text{het}}$  and the adsorption coefficient of valeric and peroxyvaleric acid  $K_{\text{VA and PVA adsorption}}^C$  were estimated by the model. Due to a similar structure of the peroxycarboxylic acid and the corresponding carboxylic acid, the adsorption coefficients  $K_{\text{VA adsorption}}^C$  and  $K_{\text{PVA adsorption}}^C$  were approximated to be equal.

The homogeneous reaction rates in the organic and aqueous phase were expressed by [9, 16]

$$r_{\text{hom,org}} = \frac{k_{\text{hom,org}} \sqrt{K_{\text{VA dissociation}}^C \times [\text{VA}]_{\text{org}} \times [\text{H}_2\text{O}]_{\text{org}}}}{[\text{H}_2\text{O}]_{\text{org}}} \times \left( [\text{VA}]_{\text{org}} \times [\text{H}_2\text{O}_2]_{\text{org}} - \frac{1}{K_{\text{hom,org}}^C} \times [\text{PVA}]_{\text{org}} \times [\text{H}_2\text{O}]_{\text{org}} \right) \quad (9)$$

$$r_{\text{hom, aq}} = \frac{k_{\text{hom, aq}} \sqrt{K_{\text{VA dissociation}}^{\text{C}} \times [\text{VA}]_{\text{aq}} \times [\text{H}_2\text{O}]_{\text{aq}}}}{[\text{H}_2\text{O}]_{\text{aq}}} \times \left( [\text{VA}]_{\text{aq}} \times [\text{H}_2\text{O}_2]_{\text{aq}} - \frac{1}{K_{\text{hom, aq}}^{\text{C}}} \times [\text{PVA}]_{\text{aq}} \times [\text{H}_2\text{O}]_{\text{aq}} \right) \quad (10)$$

where  $K_{\text{VA dissociation}}^{\text{C}}$  is the dissociation constant of valeric acid calculated based on the equation of Sue et al. [29]. The concentration of peroxyvaleric acid in the aqueous phase was too low to be detected and thus it was assumed that  $[\text{PVA}]_{\text{aq}} \approx 0$ . Consequently, eq 10 becomes:

$$r_{\text{hom, aq}} = \frac{k_{\text{hom, aq}} \sqrt{K_{\text{VA dissociation}}^{\text{C}} \times [\text{VA}]_{\text{aq}} \times [\text{H}_2\text{O}]_{\text{aq}}}}{[\text{H}_2\text{O}]_{\text{aq}}} \times \left( [\text{VA}]_{\text{aq}} \times [\text{H}_2\text{O}_2]_{\text{aq}} \right) \quad (11)$$

The kinetic parameters  $k_{\text{hom, aq}}$  and  $k_{\text{hom, org}}$  were estimated by the model. The main assumption is that the global equilibrium constants in case of the homogeneous system  $K_{\text{hom}}^{\text{C}}$  and in case of the heterogeneous system  $K_{\text{het}}^{\text{C}}$  are equal. The homogeneously catalyzed reaction was assumed to be negligible inside the particle, since the amount of liquid inside the pores is small compared to the amount of bulk liquid. Since peroxyvaleric acid is a much weaker acid than valeric acid, the contribution of peroxyvaleric acid to the homogeneous catalysis was neglected.

### 3.5. Mathematical model of the system

The goal of mathematical modelling was to establish the relation between the kinetic, thermodynamic and mass transfer parameters. As illustrated by Figure 6, hydrogen peroxide and water were assumed to diffuse from the bulk aqueous phase to the catalyst particle and from the bulk aqueous phase to the organic phase; valeric acid was assumed to diffuse from the bulk organic phase to the catalyst particle and from the bulk organic phase to the aqueous phase; the product peroxyvaleric acid was assumed to diffuse from the particle to the bulk organic phase.

#### 3.5.1 Mass balance in the aqueous phase

The mass balance of an arbitrary component (i) in the aqueous liquid phase is

$$\dot{n}(i)_{aq,in} + r_{hom, aq}(i)V_{aq} = \dot{n}(i)_{aq,out} + \frac{dn(i)_{aq}}{dt} \quad (12)$$

Because it is a batch system, thus, the inlet and outlet terms are due to the interfacial phase transfer.

The interfacial component flux  $N_X(i)$  can be expressed by the law of Fick:

$$\left. \begin{aligned} N_{org}(i) &= k_{org-i} \times ([i]_{org}^* - [i]_{org}) \\ N_{aq}(i) &= k_{aq-i} \times ([i]_{aq}^* - [i]_{aq}) \\ N_p(i) &= k_{p-i} \times ([i]_{org} - [i]_p) \text{ or } N_{p(i)} = k_{p-i} \times ([i]_{aq} - [i]_p) \end{aligned} \right\} \quad (13)$$

where  $[i]_X^*$  is the concentration at the interface from the organic or aqueous side,

$k_{X-i}$  is the mass transfer coefficient of the compound (i) in the X phase, and  $[i]_p$  is

the concentration inside the catalyst particle.

After introducing  $a_o$  as the interfacial area between the organic and aqueous phase expressed as

$$a_o = \frac{A_{aq/org}}{V_{o,tot}} \quad (14)$$

The calculation of the parameter  $a_o$  is explained in Appendix A. The mass balance of peroxyvaleric acid in the aqueous phase was not taken into account due to the absence of data, i.e., very low concentration.

The mass balance on the species present in the aqueous phase gives

$$\begin{aligned} \frac{d[VA]_{aq}}{dt} &= k_{aq-VA} \cdot a_o \cdot \frac{V_{o,tot}}{V_{aq}} \left( [VA]_{aq}^* - [VA]_{aq} \right) - r_{hom,aq} \\ \frac{d[H_2O]_{aq}}{dt} &= -k_{aq-H_2O} \cdot a_o \cdot \frac{V_{o,tot}}{V_{aq}} \left( [H_2O]_{aq} - [H_2O]_{aq}^* \right) - k_{p-H_2O} \frac{A_{b/p}}{V_{aq}} \left( [H_2O]_{aq} - [H_2O]_p \right) + r_{hom,aq} \\ \frac{d[H_2O_2]_{aq}}{dt} &= -k_{aq-H_2O_2} \cdot a_o \cdot \frac{V_{o,tot}}{V_{aq}} \left( [H_2O_2]_{aq} - [H_2O_2]_{aq}^* \right) - k_{p-H_2O_2} \frac{A_{b/p}}{V_{aq}} \left( [H_2O_2]_{aq} - [H_2O_2]_p \right) - r_{hom,aq} \end{aligned} \quad (15)$$

### 3.5.2 Mass balance of the organic phase

The mass balance of an arbitrary component (i) in the organic liquid phase is given by

$$\dot{n}(i)_{orgin} + r_{homorg}(i)V_{org} = \dot{n}(i)_{orgout} + \frac{dn(i)_{org}}{dt} \quad (16)$$

Analogously with the treatment of the aqueous phase, the mass balance of the species present in the organic phase can be written as:



$$\begin{aligned}
\frac{d[\text{VA}]_{\text{org}}}{dt} &= -k_{\text{org-VA}} a_o \cdot \frac{V_{\text{o,tot}}}{V_{\text{org}}} ([\text{VA}]_{\text{org}} - [\text{VA}]_{\text{org}}^*) - k_{\text{p-VA}} \frac{A_{\text{liq/p}}}{V_{\text{org}}} ([\text{VA}]_{\text{org}} - [\text{VA}]_{\text{p}}) - r_{\text{hom,org}} \\
\frac{d[\text{H}_2\text{O}]_{\text{org}}}{dt} &= k_{\text{org-H}_2\text{O}} a_o \cdot \frac{V_{\text{o,tot}}}{V_{\text{org}}} ([\text{H}_2\text{O}]_{\text{org}}^* - [\text{H}_2\text{O}]_{\text{org}}) + r_{\text{hom,org}} \\
\frac{d[\text{H}_2\text{O}_2]_{\text{org}}}{dt} &= k_{\text{org-H}_2\text{O}_2} a_o \cdot \frac{V_{\text{o,tot}}}{V_{\text{org}}} ([\text{H}_2\text{O}_2]_{\text{org}}^* - [\text{H}_2\text{O}_2]_{\text{org}}) - r_{\text{hom,org}} \\
\frac{d[\text{PVA}]_{\text{org}}}{dt} &= k_{\text{p-PVA}} \frac{A_{\text{liq/p}}}{V_{\text{org}}} ([\text{PVA}]_{\text{org}} - [\text{PVA}]_{\text{p}}) + r_{\text{hom,org}}
\end{aligned} \tag{17}$$

### 3.5.3 Mass balances of the solid phase

The mass balance for a compound (i) in the solid phase is

$$\dot{n}^{(i)}_{\text{p,in}} + r_{\text{het}}^{(i)} \times \varepsilon_p \times V_p = \dot{n}^{(i)}_{\text{p,out}} + \frac{dr^{(i)}_p}{dt} \tag{18}$$

where  $r_{\text{het}}$  is the reaction rate catalyzed by the resin;  $V_p$  is the volume of the catalyst particle and  $\varepsilon_p$  is the porosity of the particle.

The mass balance of the species present in the solid phase gives

$$\begin{aligned}
\frac{d[\text{VA}]_p}{dt} &= k_{\text{p-VA}} \frac{A_{\text{liq/p}}}{\varepsilon_p V_p} ([\text{VA}]_{\text{org}} - [\text{VA}]_p) - r_{\text{het}} \\
\frac{d[\text{H}_2\text{O}]_p}{dt} &= k_{\text{p-H}_2\text{O}} \frac{A_{\text{liq/p}}}{\varepsilon_p V_p} ([\text{H}_2\text{O}]_{\text{aq}} - [\text{H}_2\text{O}]_p) + r_{\text{het}} \\
\frac{d[\text{H}_2\text{O}_2]_p}{dt} &= k_{\text{p-H}_2\text{O}_2} \frac{A_{\text{liq/p}}}{\varepsilon_p V_p} ([\text{H}_2\text{O}_2]_{\text{aq}} - [\text{H}_2\text{O}_2]_p) - r_{\text{het}} \\
\frac{d[\text{PVA}]_p}{dt} &= -k_{\text{p-PVA}} \frac{A_{\text{liq/p}}}{\varepsilon_p V_p} ([\text{PVA}]_{\text{org}} - [\text{PVA}]_p) + r_{\text{het}}
\end{aligned} \tag{19}$$

The parameter  $A_{\text{liq/p}}$  is the external area of the resin particles which are in contact with the bulk-liquid mixture.

### 3.5.4 Estimation of mass transfer coefficients

Correlations found in the literature were used to estimate the different mass transfer coefficients included in the mathematical model,  $k_{org-i}$ ,  $k_{aq-i}$  and  $k_{p-i}$ .

#### *Mass transfer coefficient in the continuous organic phase*

The relation of Calderbank and Moo-Young [30] was used to estimate the value of the mass transfer coefficient in the continuous organic phase:

$$k_{c-i} = 1.3 \times 10^{-3} \left[ \frac{P\mu_c}{V_c\rho_c} \right]^{\frac{1}{4}} \left[ \frac{\mu_c}{D_{m-i}\rho_c} \right]^{\frac{-2}{3}} \quad (20)$$

where,  $\mu_c$  ( $\text{kg}\cdot\text{m}^{-1}\cdot\text{s}^{-1}$ ),  $V_c$  ( $\text{m}^3$ ) and  $\rho_c$  ( $\text{kg}\cdot\text{m}^{-3}$ ) are the viscosity, volume and density of the continuous phase, respectively; the parameter  $P$  ( $\text{kg}\cdot\text{m}^2\cdot\text{s}^{-3}$ ) is the power dissipated by the agitator and  $D_{m-i}$  ( $\text{m}^2\cdot\text{s}^{-1}$ ) is the diffusion coefficient in the multicomponent liquid mixture (Appendix B). The factor  $P$  is equal to  $P = \psi \rho_m n_a^3 D_a^5$ , where  $\psi$  is the agitator power consumption number equal to 1.5 [31],  $\rho_m$  ( $\text{kg}\cdot\text{m}^{-3}$ ) is the density of the mixture equal to  $\phi_c\rho_c + \phi_d\rho_d$ ,  $n_a$  is the stirring velocity and  $D_a$  the stirrer diameter. The viscosity of the continuous phase  $\mu_c$  ( $\text{kg}\cdot\text{m}^{-1}\cdot\text{s}^{-1}$ ) was assumed to be equal to that of valeric acid [32].

#### *Mass transfer coefficient of the dispersed aqueous phase*

The value of the mass transfer coefficient of the dispersed phase depends on the droplet behaviour: mostly upon whether the drop is rigid or not. To be able to evaluate the latter phenomenon, the diameter number ( $d^*$ ) must be calculated [33-34]:

$$d^* = d_{32} \left[ \frac{\mu_c^2}{\rho_c g \Delta \rho} \right]^{-1/3} \quad (21)$$

where  $d_{32}$  is the Sauter number (m) equal to  $\frac{\sum n_i d_i^3}{\sum n_i d_i^2}$  where  $n_i$  represents the number of drops with diameter  $d_i$ ,  $g$  is the gravity constant ( $9.81 \text{ m.s}^{-2}$ ),  $\rho_c$  the density of the continuous phase,  $\rho_d$  the density of the dispersed phase and  $\Delta \rho = \rho_c - \rho_d$ . To be considered as a rigid sphere, the value of  $d^*$  should be less than 10. Based on eq 21, it was found that the aqueous droplet can be assumed to be rigid in our system. For a rigid sphere, Treybal [35] gives the following relation:

$$k_{d-i} = \frac{2\pi^2 D_{m-i}}{3 d_{32}} \quad (22)$$

#### *Mass transfer coefficient in the particle phase*

The mass transfer coefficient in the solid can be estimated by using Kolmogoroff's theory, which assumes isotropic turbulence. The mass transfer coefficients were calculated by using the Calderbank and Jones relation [36],

$$k_{p-i} = \frac{D_{p-i}}{d_p} \left( 2 + 0.31 \left[ \frac{d_p^3 g (\rho_p - \rho_c)}{\mu_c D_{p-i}} \right]^{1/3} \right) \quad (23)$$

where  $d_p$  is the diameter of the resin particle, which was assumed to be equal to  $500 \mu\text{m}$  [16].

Figure 8 shows the value of the mass transfer coefficients in the organic phase, aqueous and solid phase with an initial weight percent of valeric acid equal to 50 wt. %.

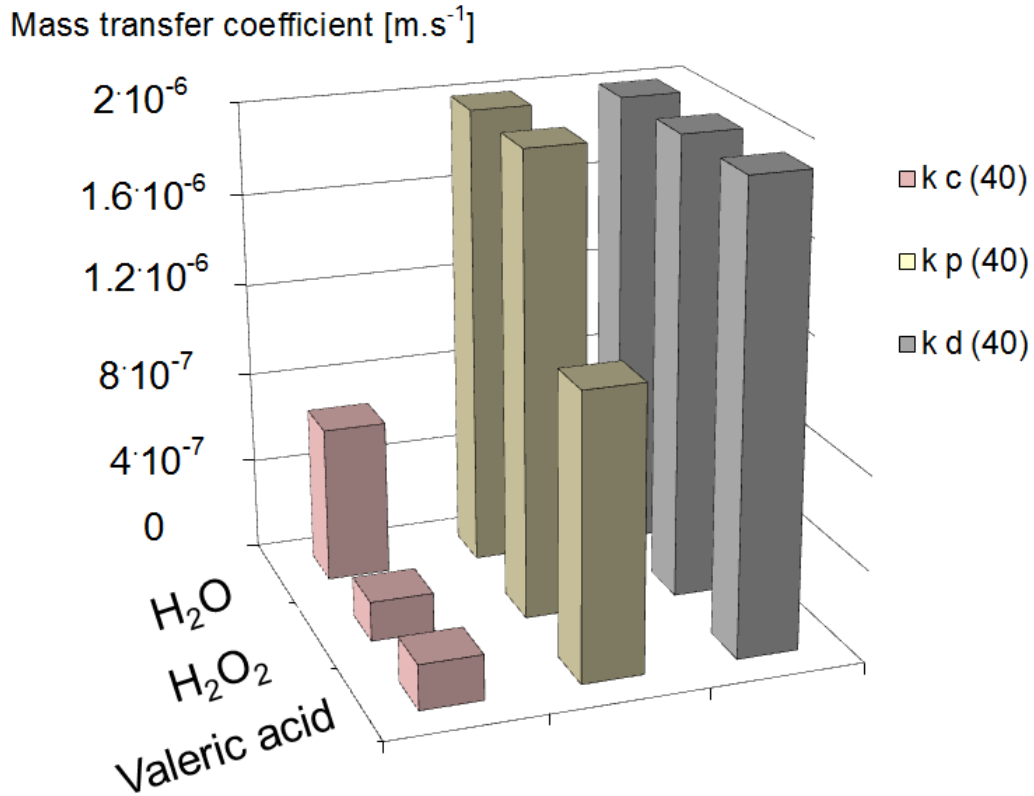


Figure 8. Mass transfer coefficients of compounds for the continuous, dispersed and particle phase at 40°C.

Figure 8 indicates that  $k_{aq-i} > k_{p-i} > k_{org-i}$ , and that the mass transfer coefficient for water is always the highest one.

### 3.5.5 Simplifications

From the different correlations used, one can notice that the mass transfer coefficients for the aqueous phase are around one hundred fold compared to those of the organic and particle phases. Thus, one can assume that there is no mass transfer resistance in the aqueous film, i.e.,  $[i]_{aq}^* \approx [i]_{aq}$ . Eq 4 becomes,

$$m(i) = \frac{[i]_{org}^*}{[i]_{aq}^*} \approx \frac{[i]_{org}^*}{[i]_{aq}} \quad (24)$$

Thus, the equation system (15) becomes,

$$\left. \begin{aligned}
\frac{d[\text{VA}]_{\text{aq}}}{dt} &= -r_{\text{hom, aq}} \\
\frac{d[\text{H}_2\text{O}]_{\text{aq}}}{dt} &= -k_{\text{p-H}_2\text{O}} \frac{A_{\text{liq/p}}}{V_{\text{aq}}} ([\text{H}_2\text{O}]_{\text{aq}} - [\text{H}_2\text{O}]_{\text{p}}) + r_{\text{hom, aq}} \\
\frac{d[\text{H}_2\text{O}_2]_{\text{aq}}}{dt} &= -k_{\text{p-H}_2\text{O}_2} \frac{A_{\text{liq/p}}}{V_{\text{aq}}} ([\text{H}_2\text{O}_2]_{\text{aq}} - [\text{H}_2\text{O}_2]_{\text{p}}) - r_{\text{hom, aq}}
\end{aligned} \right\} \quad (25)$$

And the equation system (17) becomes,

$$\left. \begin{aligned}
\frac{d[\text{VA}]_{\text{org}}}{dt} &= -k_{\text{org-VA}} a_o \cdot \frac{V_{\text{o, tot}}}{V_{\text{org}}} ([\text{VA}]_{\text{org}} - m(\text{VA}) \times [\text{VA}]_{\text{aq}}) - k_{\text{p-VA}} \frac{A_{\text{liq/p}}}{V_{\text{org}}} ([\text{VA}]_{\text{org}} - [\text{VA}]_{\text{p}}) - r_{\text{hom, org}} \\
\frac{d[\text{H}_2\text{O}]_{\text{org}}}{dt} &= k_{\text{org-H}_2\text{O}} a_o \cdot \frac{V_{\text{o, tot}}}{V_{\text{org}}} (m(\text{H}_2\text{O}) \times [\text{H}_2\text{O}]_{\text{aq}} - [\text{H}_2\text{O}]_{\text{org}}) + r_{\text{hom, org}} \\
\frac{d[\text{H}_2\text{O}_2]_{\text{org}}}{dt} &= k_{\text{org-H}_2\text{O}_2} a_o \cdot \frac{V_{\text{o, tot}}}{V_{\text{org}}} (m(\text{H}_2\text{O}_2) \times [\text{H}_2\text{O}_2]_{\text{aq}} - [\text{H}_2\text{O}_2]_{\text{org}}) - r_{\text{hom, org}} \\
\frac{d[\text{PVA}]_{\text{org}}}{dt} &= k_{\text{p-PVA}} \frac{A_{\text{liq/p}}}{V_{\text{org}}} ([\text{PVA}]_{\text{org}} - [\text{PVA}]_{\text{p}}) + r_{\text{hom, org}}
\end{aligned} \right\} \quad (26)$$

By assuming that the diffusion flux through the liquid-solid interface is identical to the chemical rate, the system of eqs 25 and 26 can now be simplified to

$$\left. \begin{aligned}
\frac{d[\text{VA}]_{\text{aq}}}{dt} &= -r_{\text{hom, aq}} \\
\frac{d[\text{H}_2\text{O}]_{\text{aq}}}{dt} &= \frac{r_{\text{het}} \cdot \varepsilon \cdot V_{\text{p}}}{V_{\text{aq}}} + r_{\text{hom, aq}} \\
\frac{d[\text{H}_2\text{O}_2]_{\text{aq}}}{dt} &= -\frac{r_{\text{het}} \cdot \varepsilon \cdot V_{\text{p}}}{V_{\text{aq}}} - r_{\text{hom, aq}}
\end{aligned} \right\} \quad (27)$$

$$\left. \begin{aligned}
\frac{d[\text{VA}]_{\text{org}}}{dt} &= -k_{\text{org-VA}} \cdot a_o \cdot \frac{V_{\text{o,tot}}}{V_{\text{org}}} \left( [\text{VA}]_{\text{org}} - m(\text{VA}) \times [\text{VA}]_{\text{aq}} \right) - \frac{r_{\text{het}} \cdot \varepsilon_p \cdot V_p}{V_{\text{org}}} - r_{\text{hom,org}} \\
\frac{d[\text{H}_2\text{O}]_{\text{org}}}{dt} &= k_{\text{org-H}_2\text{O}} \cdot a_o \cdot \frac{V_{\text{o,tot}}}{V_{\text{org}}} \left( m(\text{H}_2\text{O}) \times [\text{H}_2\text{O}]_{\text{aq}} - [\text{H}_2\text{O}]_{\text{org}} \right) + r_{\text{hom,org}} \\
\frac{d[\text{H}_2\text{O}_2]_{\text{org}}}{dt} &= k_{\text{org-H}_2\text{O}_2} \cdot a_o \cdot \frac{V_{\text{o,tot}}}{V_{\text{org}}} \left( m(\text{H}_2\text{O}_2) \times [\text{H}_2\text{O}_2]_{\text{aq}} - [\text{H}_2\text{O}_2]_{\text{org}} \right) - r_{\text{hom,org}} \\
\frac{d[\text{PVA}]_{\text{org}}}{dt} &= \frac{r_{\text{het}} \cdot \varepsilon_p \cdot V_p}{V_{\text{org}}} + r_{\text{hom,org}}
\end{aligned} \right\} \quad (28)$$

The system of eqs 27 and 28 were included in the model to estimate the kinetic parameters.

### 3.6. Kinetic modelling and results

The set of ordinary differential eqs 27 and 28 were solved out by a special software MODEST [37]. The objective function Q was minimized by using Simplex and Levenberg-Marquardt algorithms. The objective function was defined as follows  $Q = \sum (C_i - \hat{C}_i)^2$  where  $C_i$  is the experimental concentration and  $\hat{C}_i$  is the estimated concentration obtained from the model. The concentrations of VA, PVA, water and  $\text{H}_2\text{O}_2$  were included in the objective function with equal weights.

Two different models were developed, one to estimate the kinetics parameters for the homogeneously catalyzed reaction (eqs 9 and 10) and the other one to estimate the kinetic parameters for the heterogeneous reaction (eq 8).

The temperature dependences of the rate constants were described by a modified Arrhenius equation:

$$k = k_{ave} \exp\left(\frac{-Ea}{R} \left(\frac{1}{T} - \frac{1}{T_{ave}}\right)\right) \quad (29)$$

where  $k_{ave} = Ae^{-\left(\frac{Ea}{RT_{ave}}\right)}$ ,  $T_{ave}$  is the average temperature of the experiments. The goal of this modification was to minimize the correlation between the frequency factor and the activation energy during the parameter estimation.

In these models, the equilibrium parameters  $K^C$  and  $\Delta H_f$  determined in Section 3.1 were used, i.e., 2.1 at 40°C and -13.84 kJ/mol. The distribution coefficients for valeric acid, hydrogen peroxide and water were determined by using eq 6.

#### *Homogeneous catalysis*

The experiments carried out without any added catalyst were taken into account in this model. Thus, the term  $r_{het}$  disappears in the system of eqs 27 and 28. The kinetics of formation of peroxyvaleric acid in such liquid-liquid system is very slow, for that reason only the parameters  $k_{hom\_aq}$  and  $k_{hom\_org}$  were estimated and assumed to be constant in the temperature range 40-60°C.

The explanation coefficient of this model was defined by

$$R^2 = 1 - \frac{\sum (C_i - \hat{C}_i)^2}{\sum (C_i - \bar{C}_i)^2} \quad (30)$$

where  $C_i$  is the experimental concentration value,  $\hat{C}_i$  is the estimated concentration value and  $\bar{C}_i$  is the mean concentration value of the observations. The explanation coefficient of this model became 98.77 %, which shows a good agreement between the experimental and calculated values.

The results of the kinetic modelling are summarized in the Table 3.

Table 3. Estimated parameters and values of standard errors

Parameters	Estimated	Errors (%)
$k_{\text{hom\_aq}} \text{ (m}^3 \cdot \text{mol}^{-1} \cdot \text{s}^{-1}\text{)}$	$0.64 \cdot 10^{-4}$	311
$k_{\text{hom\_org}} \text{ (m}^3 \cdot \text{mol}^{-1} \cdot \text{s}^{-1}\text{)}$	$0.33 \cdot 10^{-5}$	138.3

The parameter estimation in case of reaction without catalyst is difficult due to the lack of data concerning the concentration of peroxyvaleric acid in the aqueous phase. Furthermore, the dissociation constant  $K_{\text{VA dissociation}}^{\text{C}}$  was calculated by using Sue et al. equation [29] at infinite dilution, which is not the case in the organic phase. From Figure 7, one can notice that the kinetics depends essentially on the solid acid catalyst, i.e., the heterogeneous part, thus the homogeneous part could be negligible with a certain amount of catalyst. The main goal of this article is to propose a kinetic model for such liquid-liquid-solid system.

#### *Heterogeneous catalysis*

In this model, the kinetic parameters in the presence of the heterogeneous catalyst (eq 8) were estimated by using the modified Arrhenius equation (eq 29). Two parameters were estimated, namely  $k_{\text{ave\_het}}$  and  $E_{\text{a\_het}}$ . Preliminary results from the modelling have shown that a value of  $6.19 \cdot 10^{-8} \text{ m}^3/\text{mol}$  for  $K_{\text{VA and PVA adsorption}}^{\text{C}}$  gave better statistical results. Due to the complexity to estimate this parameter, the value of  $6.19 \cdot 10^{-8} \text{ m}^3/\text{mol}$  was used.



The coefficient of explanation of this model became higher than 99%. Table 4 gives the value of the estimated parameters and the statistical data.

Table 4. Estimated parameters, values of standard errors and correlation matrix at 45°C

Parameters	Estimated	Errors (%)	Correlation matrix	
			$k_{ave\_het}$ ( $m^3 \cdot mol^{-1} \cdot s^{-1}$ )	$E_a$ ( $kJ \cdot mol^{-1}$ )
$k_{ave\_het}$ ( $m^3 \cdot mol^{-1} \cdot s^{-1}$ )	$2.72 \cdot 10^{-12}$	12.9	1	
$E_a$ ( $kJ \cdot mol^{-1}$ )	64.5	20.4	-0.456	1

The contour plot (Figure 9) shows that there is a clearly visible minimum for the activation energy and the rate constant  $k_{ave\_het}$ .

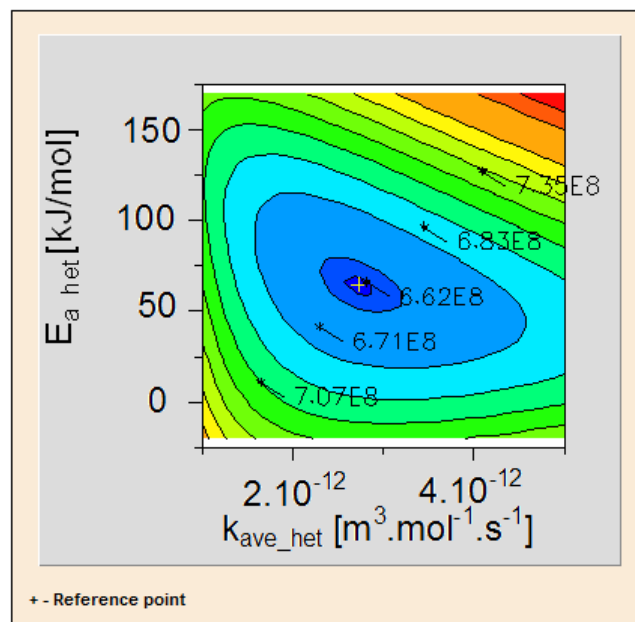


Figure 9. Contour plot of kinetic parameters.

Examples of kinetic modelling are illustrated by Figure 10.

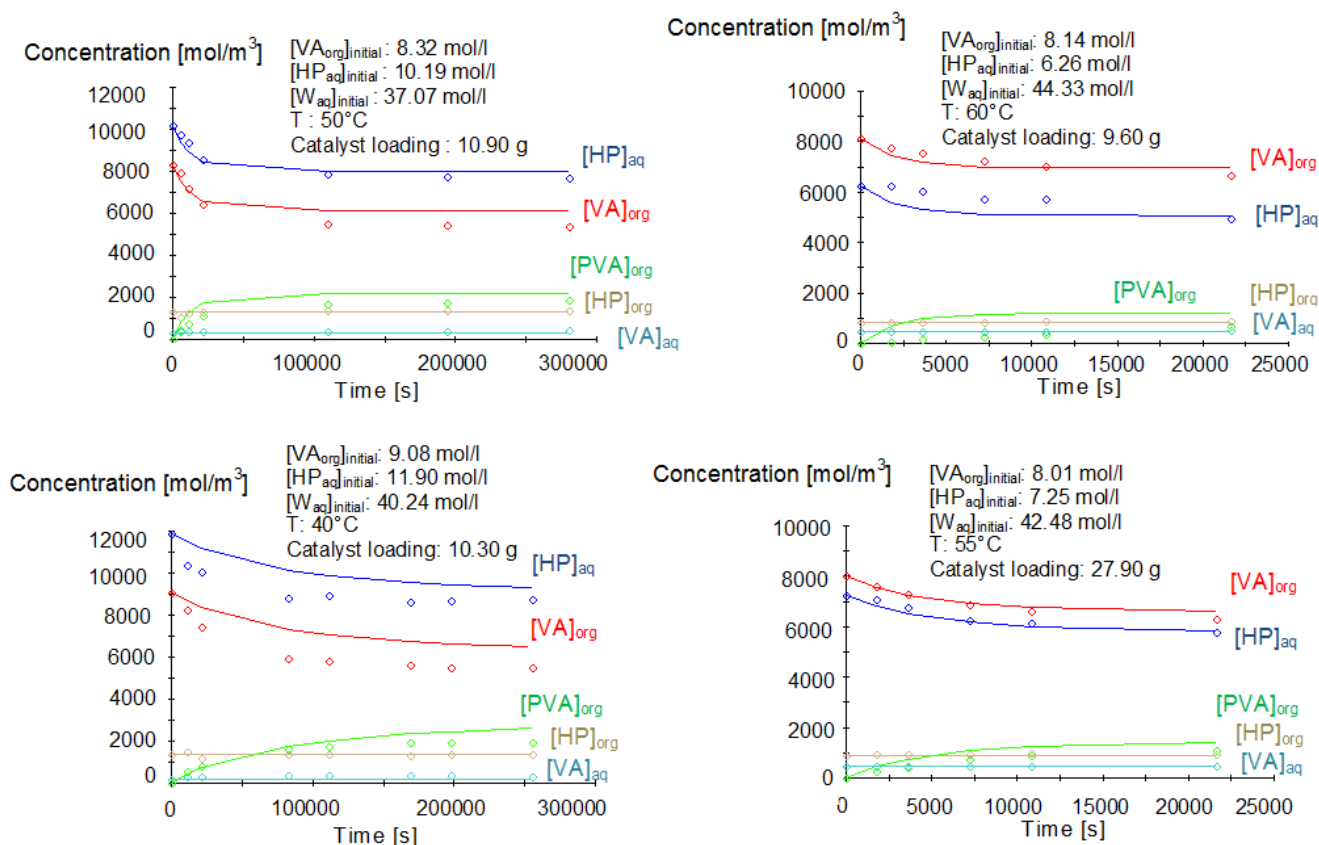


Figure 10. Fit of the model to the experiments for the perhydrolysis of valeric acid catalyzed by Amberlite IR-120.

The standard errors of the kinetic parameters were relatively low and the parameters did not correlate mutually. Figure 10 shows that the model fits properly the experimental data.

#### 4. Conclusions

The goal of this work was to develop a kinetic model for a heterogeneous liquid-liquid-solid reaction system carried out in a well-agitated batch reactor, i.e., the synthesis of peroxyvaleric acid from the parent carboxylic acid and hydrogen

peroxide by using Amberlite IR-120 as a heterogeneous catalyst in the temperature range of 40-60°C. This model is valid for a valeric acid concentration of 50 wt.%, a catalyst loading range of 0-29 g and hydrogen peroxide concentration (in the aqueous phase) in the range of 6-10.5 mol/l.

By using conductivity measurements, it was found that for an initial concentration of valeric acid exceeding 45 wt.%, the continuous phase is the organic phase.

It was observed that the conversion of valeric acid was three times higher with an initial concentration of valeric acid equal to 50 wt.% than 34 or 21 wt.%.

The thermodynamic phenomena such as equilibrium and distribution constants were studied. It was observed that both parameters follow the law of van't Hoff for the valeric acid perhydrolysis. In case of a reaction mixture with an initial concentration of 50 wt.% of valeric acid, the reaction enthalpy was found to be -13.04kJ/mol. This value shows that the reaction is slightly exothermic, similarly to the perhydrolysis of acetic and propionic acid. It was found that the distribution constant for water and hydrogen peroxide were quasi-constants in the temperature range 40-60°C and with  $[VA]_0$ : 50 wt.%.

To develop this model, it was assumed that the mass transfer resistance in aqueous film was negligible, and that mass flow through the liquid-solid interface was identical to the chemical reaction rate. In the absence of the solid catalyst, the kinetics of PVA formation was very slow and thus difficult to model quantitatively. In the presence of the cation-exchange resin, the reaction mechanism was assumed to be of Eley-Rideal type, according to which valeric acid is adsorbed on the active site. It was possible to develop a model, which takes into account the concentrations inside the catalyst particle, as well as the phase transfer and equilibrium phenomena.

## NOTATION

A	pre-exponential factor [ $\text{l.mol}^{-1}.\text{s}^{-1}$ ]
A	interfacial area [ $\text{m}^2$ ]
a	activity of compounds
$a_o$	interfacial area-to-liquid volume [ $\text{m}^{-1}$ ]
C	concentration
$d^*$	diameter number
$d_{32}$	Sauter number [m]
$d_p$	diameter of the resin particle
$D_i$	molecular diffusion coefficient [ $\text{m}^2.\text{s}^{-1}$ ]
$De_i$	effective diffusion coefficient [ $\text{m}^2.\text{s}^{-1}$ ]
Ea	activation energy [ $\text{kJ.mol}^{-1}$ ]
k	rate constant [ $\text{l.mol}^{-1}.\text{s}^{-1}$ ]
K	adsorption coefficient [ $\text{l.mol}^{-1}$ ]
k	mass transfer coefficient [ $\text{m.s}^{-1}$ ]
$K^c$	equilibrium constant, based on concentrations
$K^T$	true thermodynamic constant, based on activities
$\dot{n}$	flow of the amount of substance [ $\text{mol.s}^{-1}$ ]
n	amount of substance [mol]
n	number of drops
N	flux [ $\text{mol.m}^{-2}.\text{s}^{-1}$ ]
P	power dissipated by the agitator [ $\text{kg}.\text{(s}^3\text{m}^2\text{)}^{-1}$ ]

Q	objective function
R	gas constant [ $\text{J.K}^{-1}.\text{mol}^{-1}$ ]
$R^2$	coefficient of explanation [%]
r	catalyst particle radius, radial coordinate
$r_i$	generation rate
$r_j$	particle radius
$\bar{r}$	average radius
T	temperature [K]
V	volume
We	Weber number
y	frequency function for particle size distribution
X	dimensionless coordinate
$\Delta H_r^\circ$	standard enthalpy change of reaction [ $\text{kJ}.\text{mol}^{-1}$ ]
$\Delta H_f^\circ$	heat of formation of specie [ $\text{kJ}.\text{mol}^{-1}$ ]
$\Delta G_d$	Gibbs energy of distribution [ $\text{kJ}.\text{mol}^{-1}$ ]

## Greek letters

$\alpha$	organic species coefficient of absorption
$\Upsilon$	interfacial surface tension [N/m]
$\beta$	aqueous species coefficient of absorption
$\varepsilon_p$	porosity of particle
$\mu$	viscosity [ $\text{kg}\cdot\text{m}^{-1}\cdot\text{s}^{-1}$ ]
$\rho_p$	density of particle
$\sigma$	surface tension [ $\text{N}\cdot\text{m}^{-1}$ ]
$\tau_p$	tortuosity of particle
$\varphi$	agitator power consumption number
$\Phi$	association factor
$\Phi_d$	fraction of dispersed phase

## Subscripts

c	continuous phase
d	dispersed phase
p	solid phase
aq	aqueous phase
ave	average
eq	equilibrium
het	heterogeneous catalytic system
hom	homogeneous catalytic system
org	organic phase
ref	reference state
<i>i</i>	component <i>i</i>
0	initial
*	interfacial value

## Abbreviations

VA	valeric acid
PVA	peroxyvaleric acid

## **ACKNOWLEDGEMENTS**

This work is part of the activities at the Åbo Akademi Process Chemistry Centre (PCC) within the Finnish Centre of Excellence Programme (2006-2011) by the Academy of Finland.



## APPENDIX

### A. Calculation of interfacial area between the organic and the aqueous phase ( $a_o$ )

The interfacial area was calculated using the following expression [27, 33, 38]:

$$a_o = \frac{6\Phi_d}{d_{32}} \quad (\text{A.1})$$

where  $\Phi_d$  is the fraction of dispersed phase (here: aqueous phase),  $d_{32}$  is the

Sauter number (m) equal to  $\frac{\sum n_i d_i^3}{\sum n_i d_i^2}$  where  $n_i$  represents the number of droplets

with diameter  $d_i$ .

The Sauter number  $d_{32}$  can be calculated as [38]:

$$\frac{d_{32}}{D_a} = \frac{Af(\Phi_d)}{We^{0.6}} \quad (\text{A.2})$$

where  $D_a$  is the stirrer diameter (4 cm),  $A$  is a parameter varying between 0.04 and 0.4[38].

The Weber number ( $We$ ) is expressed as:

$$We = \frac{\rho_c n_a^2 D_a^3}{\sigma} \quad (\text{A.3})$$

where  $\rho_c$  is the density of the continuous phase ( $\text{kg}\cdot\text{m}^{-3}$ ) (here: organic phase) ( $969 \text{ kg}/\text{m}^3$ ),  $n_a$  is the stirring velocity ( $\text{s}^{-1}$ ), (here:  $n_a = 6.16 \text{ s}^{-1}$ ),  $\sigma$  is the surface tension ( $\text{N}\cdot\text{m}^{-1}$ ) of the system.

The function  $f(\Phi_d)$  [39] is equal to

$$f(\Phi_d) = \left[ \frac{\ln(C_2 + C_3\Phi_d)}{\ln C_2} \right]^{-3} \quad (\text{A.4})$$

where  $C_2$  is equal to 0.011 and  $C_3 \rightarrow 1$  in case of  $\phi_d > 0.3$ . This function can be represented in two ways, both of which account for re-dispersion and coalescence effects.

#### *Calculation of the surface tension*

The interfacial surface tension was calculated by using the model of Good and Girifalco [40]:

$$\sigma = \gamma_c + \gamma_d - 2\phi\sqrt{\gamma_c\gamma_d} \quad (\text{A.5})$$

where  $\gamma_c$  and  $\gamma_d$  are the surface tensions of the phase. For the sake of simplicity, the surface tension of the continuous phase was supposed to be the same as that of valeric acid, and the one for the aqueous phase was supposed to be the same as that of hydrogen peroxide [32],

$$\gamma_c [N/m] = \frac{56.8}{1000} \times \left(1 - \frac{T[K]}{651}\right)^{1.2257} \quad (\text{A.6})$$

$$\gamma_d [N/m] = \frac{141.031}{1000} \times \left(1 - \frac{T[K]}{730.15}\right)^{1.2222} \quad (\text{A.7})$$

$\phi$  is the interaction parameter calculated from the average of molar volumes of continuous phase ( $V_{m,c}$ ) and dispersed phase ( $V_{m,d}$ ):

$$\phi = \frac{4 \times [V_{m,c} V_{m,d}]^{\frac{1}{3}}}{[V_{m,c}^{1/3} + V_{m,d}^{1/3}]^2} \quad (\text{A.8})$$

At 40°C, the interfacial surface area can be estimated to 0.019 N/m for the perhydrolysis of valeric acid.

## B. Estimation of diffusion coefficients in mixed solvents

In a liquid-liquid system, the diffusion coefficient of the solute can be estimated by the equation of Perkins-Geankoplis [41],

$$D_{m-i}^0 \mu_m^{0.8} = \sum_{\substack{X=1 \\ X \neq A}} x_X D_{X-i}^0 \mu_X^{0.8} \\ = x_{org} D_{org-i}^0 \mu_{org}^{0.8} + x_{aq} D_{aq-i}^0 \mu_{aq}^{0.8} \quad (B.1)$$

where  $D_{m-i}^0$  and  $D_{X-i}^0$  in eq B.1 are the diffusion coefficients in the mixed solvent and in the pure solvent, respectively. The viscosity of the solution in eq B.1 is calculated from eq B.2,

$$\ln \mu_m = \sum_{i=1}^n x_i \ln \mu_i \\ = x_{org} \ln \mu_{org} + x_{aq} \ln \mu_{aq} \quad (B.2)$$

For the sake of simplicity, the viscosity of the organic and aqueous were assumed to be equal to the viscosity of water and valeric acid [32]

Based on the study of Liu et al. [43], the correlation of Hayduk-Laudie [44] can be used to calculate the diffusion coefficients of the components in the aqueous phase (eq B.3), and the correlation of Scheibel [45] (eq B.4) to calculate the diffusion coefficients of the component in the organic phase:

$$D_{X-i}^0 [\text{cm}^2 \text{s}^{-1}] = D_{aq-i}^0 [\text{cm}^2 \text{s}^{-1}] = \frac{13.26 10^{-5}}{\mu_{aq}^{1.4} [\text{cP}] V_i^{0.589} [\text{cm}^3 \text{mol}^{-1}]} \quad (B.3)$$

$$D_{X-i}^0 [\text{cm}^2 \text{s}^{-1}] = D_{org-i}^0 [\text{cm}^2 \text{s}^{-1}] = \frac{8.2 \times 10^{-8} T [\text{K}]}{\mu_{org} [\text{cP}] V_i^{\frac{1}{3}} [\text{cm}^3 \text{mol}^{-1}]} \times \left[ 1 + \left( \frac{3V_{org} [\text{cm}^3 \text{mol}^{-1}]}{V_i [\text{cm}^3 \text{mol}^{-1}]} \right)^{\frac{2}{3}} \right] \quad (B.4)$$

where  $V_i$  is the molar volume at boiling point of the solute.

### *Estimation of the diffusion coefficients in the catalyst particle*

The diffusion coefficients of the compounds in the particle were estimated by using the equation from the random pore model,

$$D_a = \left( \frac{\varepsilon_p}{\tau_p} \right) D_i \quad (\text{B.5})$$

where  $\varepsilon_p$  is the porosity of the material equal to 0.5 and  $\tau_p$  is the tortuosity factor, which was estimated to be 2.2 according to ref. [16].  $D_i$  is the molecular diffusion coefficient for a component (i) and it was determined by using Wilke-Chang equation [42],

$$D_{X-i}^0 [\text{m}^2 \text{s}^{-1}] = D_{p-i}^0 [\text{cm}^2 \text{s}^{-1}] = \frac{7.4 \cdot 10^{-12} T [\text{K}]}{\mu_B [\text{cP}] V_i^0 [\text{cm}^3 \text{mol}^{-1}]} \left[ \Phi M_B [\text{g.mol}^{-1}] \right]^{0.5} \quad (\text{B.6})$$

where  $\Phi$  is the association factor (equal to 2.6 in case of water as solvent),  $M_B$  and  $\mu_B$  denote the molar mass and viscosity of the solvent, which is water [32]. The molar volumes were calculated from the atomic increments of Le Bas.

Diffusion coefficient [ $\text{m}^2 \cdot \text{s}^{-1}$ ]

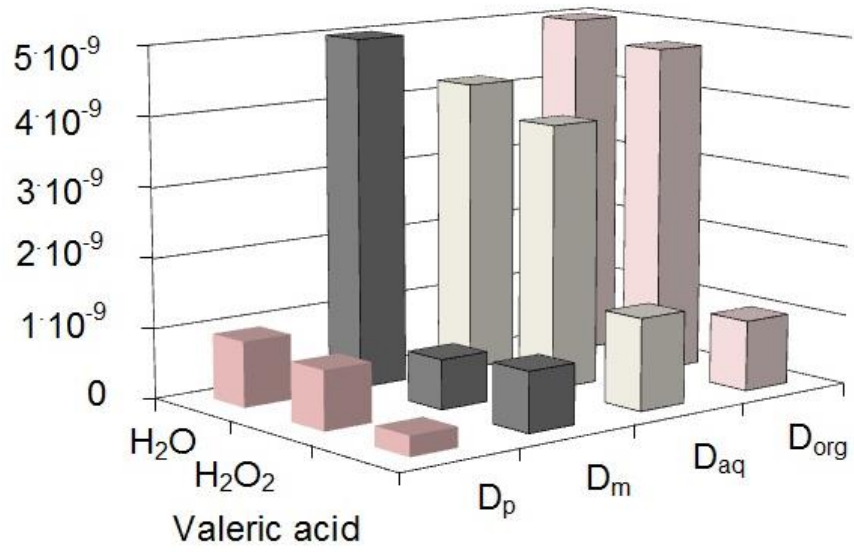


Figure B.1. Diffusion coefficients of the compounds in the pores of the solid phase  $D_p$ , in the multicomponent liquid mixture  $D_m$ , in the aqueous phase  $D_{\text{aq}}$  and in the organic phase  $D_{\text{org}}$  at  $40^\circ\text{C}$ .

## REFERENCES

- (1) Rüschen, Klaas, M.; Steffens, K.; Patett, N. Biocatalytic Peroxy Acid Formation for Disinfection. *J. Mol. Catal. B-Enzym.* **2002**, *19-20*, 499-505.
- (2) D'Ans, J.; Frey, W. Untersuchungen über die Bildung von Persäuren aus organischen Säuren und Hydroperoxyd. *Z. Anorg. Chem.* **1914**, *84*, 145-164.
- (3) Swern, D. *Organic Peroxides*; Wiley-Interscience: New York, 1970.
- (4) Dul'neva, L. V.; Moskvina, A. V. Kinetics of Formation of Peroxyacetic Acid. *Russ. J. Gen. Chem.* **2005**, *75*, 1125-1130.
- (5) Ogata, Y.; Sawaki, Y. Kinetics of the Acid-Catalysed Formation of Aliphatic Peracids from Hydrogen Peroxide and Aliphatic Acids in Dioxan. *Tetrahedron* **1965**, *21*, 3381-3386.
- (6) Zhao, X.; Zhang, T.; Zhou, Y.; Liu, D. Preparation of Peracetic Acid from Hydrogen Peroxide: Part I: Kinetics for Peracetic Acid Synthesis and Hydrolysis. *J. Mol. Catal. A-Chem.* **2007**, *271*, 246-252.
- (7) Reijo, A.; Renvall, I. Process for the Preparation of Peroxy Acids. No. WO2007031596, 2007.
- (8) Zhou, Z. X. Method for Preparing Peroxy Acetic Acid. No. CN1803771, 2006.
- (9) Leveneur, S.; Salmi, T.; Murzin, D.; Estel, L.; Warna, J.; Musakka, N. Kinetic Study and Modeling of Peroxypropionic Acid Synthesis from Propionic Acid and Hydrogen Peroxide Using Homogeneous Catalysts. *Ind. Eng. Res.* **2008**, *47*, 656-664.
- (10) Saha, M. S.; Nishiki, Y.; Furuta, T.; Denggerile, A.; Ohsaka, T. A New Method for the Preparation of Peroxyacetic Acid Using Solid Superacid Catalysts. *Tetrahedron Lett.* **2003**, *44*, 5535-5537.

- (11) Hawkinson, A.T.; Schitz, W. R. Improvements in or Relating to the Oxidation of Aliphatic Carboxylic Acids to Peracids. GB776758, 1957.
- (12) Palani, A.; Pandurangan, A. Single Pot Synthesis of Peroxyacetic Acid from Acetic Acid and Hydrogen Peroxide Using Various Solid Acid Catalysts. *Catal. Commun.* **2006**, *7*, 875-878.
- (13) Rocha, G. O.; Johnstone, R. A.; W. Hemming, B. F.; Pires, P. J. C.; Sankey, J. P. Rates of Formation of Peroxyacetic Acid from Hydrogen Peroxide and Acetic Acid in the Presence of Metal(IV) Phosphates. *J. Mol. Catal. A: Chem.* **2002**, *186*, 127-133.
- (14) Musante, R. L.; Grau, R. J.; Baltanás, M. A. Kinetic of Liquid-Phase Reactions Catalyzed by Acidic Resins: the Formation of Peracetic Acid for Vegetable Oil Epoxidation. *Appl. Catal. A* **2000**, *197*, 165-173.
- (15) Leveneur, S.; Kumar, N.; Salmi, T.; Murzin, D. Yu. Stability of Hydrogen Peroxide during Perhydrolysis of Carboxylic Acids on Acidic Heterogeneous Catalysts. *Res. Chem. Intermed.* **2010**, *36*, 389-401.
- (16) Leveneur, S.; Wärnå, J.; Salmi, T.; Murzin, D. Yu.; Estel, L. Interaction of Intrinsic Kinetics and Internal Mass Transfer in Porous Ion-Exchange Catalysts: Green Synthesis of Peroxycarboxylic Acids. *Chem. Eng. Sci.* **2009**, *64*, 4101-4114.
- (17) Leveneur, S.; Murzin, D. Yu.; Salmi, T.; Mikkola, J.-P.; Kumar, N.; Eränen, K.; Estel, L. Synthesis of Peroxypropionic Acid from Propionic Acid and Hydrogen Peroxide over Heterogeneous Catalysts. *Chem. Eng. J.* **2009**, *147*, 323-329.
- (18) Leveneur, S.; Murzin, D. Yu.; Salmi, T. Application of Linear Free-Energy Relationships to Perhydrolysis of Different Carboxylic Acids over Homogeneous and Heterogeneous Catalysts. *J. Mol. Catal. A: Chem.* **2009**, *303*, 148-155.

- (19) Yamaguchi, S.; Yamaguchi, N.; Aoyagi, M.; Ushio, N.; Tamura, S.; Tsumadori, M. Bleaching detergent Composition. US 6159919, 1996.
- (20) Amin, N. S.; Bott, R. R.; Cervin, M. A.; Poulouse, A. J.; Weyler, W. Enzyme for the Production of Long Chain Peracid, US 7754460, 2010.
- (21) Noyori, R. Pursuing Practical Elegance in Chemical Synthesis. *Chem. Commun.* **2005**, 1807-1811.
- (22) Greenspan, F. P.; MacKellar, D. G. Analysis of Aliphatic Per Acids. *Anal. Chem.* **1948**, *20*, 1061-1063.
- (23) Bucalá, V.; Foresti, M. L.; Trubiano, G.; Ferreira, M. L.; Briozzo, M.; Bottini, S. Analysis of Solvent-Free Ethyl Oleate Enzymatic Synthesis at Equilibrium Conditions. *Enzyme Microb. Tech.* **2006**, *38*, 914-920.
- (24) Zwietering, T. N. Suspending of Solid Particles in Liquid by Agitators. *Chem. Eng. Sci.* **1958**, *8*, 244-253.
- (25) Pangarkar, V. G.; Yawalkar, A. A.; Sharma, M. M.; Beenackers, A. A. C. M. Particle-Liquid Mass Transfer Coefficient in Two-/Three-Phase Stirred Tank Reactors. *Ind. Eng. Res.* **2002**, *41*, 4141-4167.
- (26) Levins, D. M.; Glastonbury, J. R. Particle Liquid Hydrodynamics and Mass Transfer in a Stirred Vessel, Part 1. Particle Liquid Motion. *Trans. Inst. Chem. Eng.* **1972**, *50*, 132-146.
- (27) Campanella, A.; Baltanás, M. A. Degradation of the Oxirane Ring of Epoxidized Vegetable Oils in a Liquid-Liquid-Solid Heterogeneous Reaction System. *Chem. Eng. Process.* **2007**, *46*, 210-221.
- (28) Altıokka, M. R.; Hoşgün, H. L. Kinetics of Hydrolysis of Benzaldehyde Dimethyl Acetal over Amberlite IR-120. *Ind. Eng. Res.* **2007**, *46*, 1058-1062.
- (29) Sue, K.; Ouchi, F.; Minami, K.; Arai, K. Determination of Carboxylic Acid



Dissociation Constants to 350 °C at 23 MPa by Potentiometric pH Measurements. *J. Chem. Eng. Data* **2004**, *49*, 1359-1363.

(30) Calderbank, P. H.; Moo-Young, M. B. The Continuous Phase Heat and Mass Transfer Properties of Dispersions. *Chem. Eng. Sci.* **1961**, *16*, 39-54.

(31) Houcine, I.; Plasari, E.; David, R. Effects of the Stirred Tank's Design on Power Consumption and Mixing Time in Liquid Phase. *Chem. Eng. Technol.* **2000**, *23*, 605-613.

(32) Yaws, C. L. *Chemical properties handbook*; McGraw-Hill: New York 1999.

(33) van Woezik, B. A. A.; Westerterp, K. R. Measurement of Interfacial Areas with the Chemical Method for a System with Alternating Dispersed Phases. *Chem. Eng. Process.* **2000**, *39*, 299-314.

(34) Wesselingh, J. A. The velocity of Particles, Drops and Bubbles. *Chem. Eng. Process.* **1987**, *21*, 9-14.

(35) Treybal, R. E. *Liquid extraction*; second ed., McGraw-Hill: New York 1963.

(36) Calderbank, P. H.; Jones, S. J. R. Physical Rate Processes in Industrial Fermentation-Part III: Mass Transfer from Fluids to Solid Particles Suspended in Mixing Vessels, *Trans. Inst. Chem. Engrs.* **1961**, *39*, 363-368.

(37) Haario, H. *MODEST-User's Guide*; Profmath Oy: Helsinki 1994.

(38) Zaldivar, J.; Molga, E.; Alos, M.; Hernandez, H.; Westerterp, K. Aromatic Nitrations by Mixed Acid. Fast Liquid-Liquid Reaction Regime. *Chem. Eng. Process.* **1996**, *35*, 91-105.

(39) Delichatsios, M. A.; Probstein, R. F. The Effect of Coalescence on the Average Drop Size in Liquid-Liquid Dispersions. *Ind. Eng. Chem. Fundam.* **1976**, *15*, 134-138.

- (40) Good, R. J.; Girifalco, L. A. A Theory for Estimation of Surface and Interfacial Energies. III. Estimation of Surface Energies of Solids from Contact Angle. *J. of Phys. Chem.* **1960**, *64*, 561-565.
- (41) Perkins, L. R.; Geankoplis, C. J. Molecular Diffusion in a Ternary Liquid System with the Diffusing Component Dilute. *Chem. Eng. Sci.* **1969**, *24*, 1035-1042.
- (42) Salmi, T. O.; Mikkola, J.-P.; Wärnå, J. *Chemical reaction engineering and reactor technology*; 1st Ed. CRC Press: 2010.
- (43) Liu, J. G.; Luo, G. S.; Pan, S.; Wang, J. D. Diffusion Coefficients of Carboxylic Acids in mixed Solvents of Water and 1-Butanol. *Chem. Eng. Process.* **2004**, *43*, 43-47.
- (44) Hayduk, W.; Laudie, H. Prediction of Diffusion Coefficients for Nonelectrolytes in Dilute Aqueous Solutions. *AIChE J.* **1974**, *20*, 611-615.
- (45) Scheibel, E. G. Correspondence: Liquid Diffusivities. Viscosity of Gases. *Ind. Eng. Chem.* **1954**, *46*, Chem. Eng. Process. 2007-2008.

